Energy and Buildings 113 (2016) 189–201

Contents lists available at ScienceDirect

Energy and Buildings

journal homepage: www.elsevier.com/locate/enbuild

Performance evaluation of building integrated solar thermal shading system: Building energy consumption and daylight provision

Li Li, Ming Qu*, Steve Peng

School of Civil Engineering, Purdue University, 550 Stadium Mall Dr. CIVL G243, West Lafayette, IN, United States

ARTICLE INFO

Article history:
Received 20 September 2015
Received in revised form
21 December 2015
Accepted 22 December 2015
Available online 25 December 2015

Keywords:
BISTS
Louver shading
Energy savings
Daylighting

ABSTRACT

This paper evaluated the performance of the building integrated solar thermal shading (BISTS) system on building energy consumption and daylight levels through energy and daylighting modeling and simulations. A medium office reference building in Los Angeles defined by the DOE was used in the case studies. The horizontal BISTS louvers on the south windows and vertical BISTS louvers on the east and west windows were modeled and simulated. The final BISTS configuration was achieved by considering the balance between primary energy savings and daylight provision. The results revealed that 1) the BISTS system could effectively improve the daylight condition for a single perimeter room by increasing the useful daylight level and reducing the excessive level. 2) The savings for the building energy consumption were not significant. The final design with the BISTS layouts on three façades could result in 5.3% of total primary energy saving. 3) 90° of slat angle should be avoided for both the horizontal and vertical BISTS louvers. Smaller angles – between 0° and 60° – are preferred.

1. Introduction

Building integrated solar thermal shading (BISTS) system is a new type of solar thermal application that potentially replaces traditional building exterior shading devices with small-sized solar thermal collectors for thermal heat generation, solar gain reduction, and glare protection. It represents a new tendency in the building sector as it could be a replacement of the traditional building elements, thus, to serve dual functions with a high esthetic value and reduce total cost [1]. In the United States, buildings are responsible for 41% of the country's primary energy use. Of all the energy consumed by buildings, space heating, space cooling, water heating, and lighting account for over 60% [2]. The BISTS system is attracting increasing interests as a new solution to reduce fossil fuel consumption and greenhouse gas emissions of buildings by taking advantage of the renewable solar energy. On the other hand, the impact to the interior daylight condition is also a constructive factor of the BISTS application.

However, studies of the BISTS system have not been widely reported [3]. The majority of existing solar thermal collectors are integrated to roofs [4,5], façades [6,7], and gutters [8–10]. Little attention was given to the shading devices. The main reason is that the traditional solar thermal collectors are heavy and large, thus it is not easy to be integrated as a shading device in terms of esthetic and structural consideration. Palmero-Marrero et al. [11] investigated the integration of solar collectors into the external louvers of a single-zone building for different climates. The building energy requirements and temperature behaviors were calculated, and the solar thermal system for water heating was evaluated [12]. Significant energy savings and solar fractions were observed. However, this study did not assess the daylighting condition. The energy analysis did not take artificial lighting into account. And only the south-oriented horizontal louvers were considered for the water heating system.

As a passive design strategy, shading system plays an important role in building energy consumption and interior visual comfort. Both energy use and visual/thermal comfort are crucial issues because energy use is related to economic and environmental factors, while comfort affects occupants' wellbeing and productivity in a building [13]. Therefore, coupling between energy and daylighting simulation is necessary for a comprehensive analysis [14]. At present, building energy performance can be effectively predicted by using building energy simulation program such as EnergyPlus, TRNSYS, and ESP-r. And many empirical methods for daylighting study in buildings have been developed and incorporated into simulation tools such as Ecotect, RADIANCE and DAYSIM [15].

Different shading types such as overhangs, louvers, roller shades, and venetian blinds have different effects on building energy consumption and daylighting condition. Mandalaki et al. [16,17] evaluated thirteen types of fixed shading systems with

* Corresponding author.
E-mail address: mqu@purdue.edu (M. Qu).

http://dx.doi.org/10.1016/j.enbuild.2015.12.040
0378-7788/

integrated PV facing south for a typical office unit in Mediterranean countries. Energy consumption for heating, cooling, and lighting was calculated; and daylight autonomy, useful daylight illuminance, and daylight glare index were used as indicators to assess the visual comfort condition. The shading performance was finally evaluated based on three basic categories: Best-Middle-Low. This study employed fixed shading dimensions from an existing project [18]. However, the variation of geometry and position will also influence the shading performance. Manzan [19] presented a genetic optimization for the design of a shading device on an office room with a south facing window. An optimization tool modeFRONTIER was used to optimize the shading parameters: height, width, angle and distance from the wall. Primary energy consumption for heating, cooling, and lighting was computed in ESP-r and the $UDI_{100–2000}$ level was calculated in DAYSIM. In order to achieve desirable energy and daylighting performances, shading and glazing properties also play important roles. Shen et al. [20] investigated the influence of glazing properties, shading properties and controls, climates, and window orientations for a perimeter private office with interior roller shades, using the maximum $UDI_{500–1000}$ index and minimum source energy consumption as the two basic criteria to balance daylighting benefits and energy requirements. Dynamic shading control was also included in this analysis and the control was based on a solar incident set-point on the façade. More shading control methods were discussed by Chan et al. [21]. Four types of venetian blind control strategies were developed considering daylight provision, lighting energy use and visual comfort. A hybrid ray-tracing and radiosity approach [22] was used to calculate the interior illuminance distributions. Daylight autonomy, useful daylight illuminance, and daylight glare probability were computed.

Most shading studies were based on a single room. This would potentially result in significant energy savings from shading applications because the thermal loads of a small building are dominated by the weather condition. This paper presents an evaluation of the BISTS system on energy and daylighting performances based on a three-story building. Both horizontal and vertical shading layouts were considered and different BISTS configurations were investigated to determine the best final design. Energy consumption for heating, cooling, and lighting were calculated. Useful and excessive daylight levels were examined. The outcomes of this study may be used to provide guidance for the BISTS louver configuration design and benefits prediction.

2. Research approach and methodology

The research aimed to evaluate the performance of the BISTS system on building energy consumption and daylight provision. The evaluation was conducted through case studies in which the BISTS were applied to a medium office reference building from the U.S. Department of Energy (DOE) [23]. DOE has developed and maintained a suite of 16 prototype building models that represent approximately 70% of the commercial buildings across 16 locations, which represent all U.S. climate zones. The medium office reference building complies with the minimum requirements of ANSI/ASHRAE/IES Standard 90.1-2010, including the envelope, lighting, heating, ventilation and air conditioning systems [24], which provides a consistent baseline of comparison for this study. Different BISTS configurations and orientations were considered in case studies and the most efficient BISTS system design was discussed by considering the balance between energy and daylighting performances. The final design would be further used to predict the active solar energy contribution to building domestic hot water (DHW) and space heating/cooling.

Energy consumption for the space cooling, space heating, and artificial lighting were predicted by using EnergyPlus simulation. EnergyPlus is an energy analysis and thermal load simulation program that is able to predict building heating and cooling loads, coil loads, and the energy consumption of primary plant equipment [25]. Primary energy (or source energy) has been used in the study as a single common unit to estimate the total energy savings from different forms of energy, including electricity and natural gas. Primary energy is the energy embodied in natural resources prior to undergoing any human-made conversions or transformations. It incorporates all transmission, delivery, and production losses, thus representing the total amount of raw fuel that is consumed by the building. The US Environmental Protection Agency has determined source energy as the most equitable unit of evaluation [26]. In this study, the conversion factors from site energy to primary energy were 3.095 for electricity and 1.092 for natural gas.

Daylight level is analyzed by using a single perimeter room, which is extracted from the reference building. Useful daylight level and excessive daylight level were estimated by DAYSIM simulation. DAYSIM is a validated [27], RADIANCE-based daylighting analysis software that models the annual amount of daylight in and around buildings. It generates climate-based daylighting metrics such as daylight autonomy, useful daylight illuminance, annual glare and electric lighting energy use [28]. In this study, Useful Daylight Illuminance (UDI) was calculated. UDI, proposed by Mardaljevic and Nabil in 2005 [29,30], is a dynamic daylight performance measure that is based on work plane illuminances. It defines the percentage of the occupied times of the year that the interior illuminance falls into three standard bins: less than 100 lx is insufficient daylight; between 100 lx and 2000 lx is useful daylight; more than 2000 lx is too much daylight and can result in visual and thermal discomfort. Nowadays the light level for normal activities is recommended in the range of 500–1000 lx [31]. Therefore $UDI_{500–1000}$ was considered as the useful daylight metric in this study and $UDI_{>2000}$ was used to reflect the excessive daylight level. The occupied hours were from 8:00 to 17:00.

3. BISTS design and configuration

3.1. BISTS prototype introduction

The solar collectors studied in this research are designed to replace the traditional shading louvers, thus to serve multiple functions. The potential markets of this application can be residential buildings, commercial buildings, and outdoor constructions. The prototype panel is 210 mm wide and 51.5 mm thick, and the length can be customized. The main housing is made of 2 mm polycarbonate, and the top and bottom surfaces are oval curved. The panel core is 10 mm thick for fluid flow through. The lower portion has 25 mm polyurethane foam insulation, whose heat conductivity is 0.03 W/m K. The upper portion has 10 mm air layer. The overall absorptivity, reflectivity, and transmissivity of the panels are 96%, 4%, and 0, respectively.

3.2. BISTS configuration

Shading devices are installed according to the orientation of the window. For the Northern Hemisphere, the horizontal shading devices can considerably reduce solar heat gains on south, southeast and southwest exposures in summer. But for the windows oriented at east and west, horizontal shadings have to be excessively long. On the other hand, the vertical shading devices are more effective for the eastern/western windows [11]. Therefore, in this study, the BISTS louvers are assumed to be installed horizontally on the south façade and vertically on the east and west facades. The northern windows were not shaded by the BISTS system. For simplification, the BISTS panel surfaces were considered as flat during

the modeling process. The space between two adjacent panels was designed to be 0.21 m to allow the louvers to be completely closed at certain slat angles. Four slat angles – 0°, 30°, 60°, and 90° – were studied.

3.2.1. Horizontal installation

The design of the horizontal BISTS is similar to the one for overhangs. Fig. 2(a) shows the configuration of horizontal BISTS system. The total depth of the BISTS d and the height above the window h were used for the design of BISTS, so that the solar radiation can come through the window during the winter and be blocked in the summer. With a given window height H, which equals to 1.3 m in this case, the d and h can be determined according to the summer and winter solar altitudes from Eqs. (1) and (2).

$$\tan\alpha_w = \frac{h}{d} \quad (1)$$

$$\tan\alpha_s = \frac{h+H}{d} \quad (2)$$

where α_w: winter solar altitude [°]; α_s: summer solar altitude [°]; d: horizontal depth of the BISTS [m]; h: vertical height of the BISTS above the window [m].

Typically summer solar altitude α_s, or winter solar altitude α_w, is determined on the basis of the summer or winter solstices, when the sun is located at its highest or lowest point in the sky at noon of the longest or shortest day. Raeissi et al. [32] used the longest day of the year, June 21st, and the shortest day, December 21st, to identify summer and winter solar altitudes. However, since the building thermal loads are not only related to the solar radiation, but also associated with the ambient temperature, façade construction, material properties, etc., they may not reach the peaks on these two days. Palmero-Marrero et al. [11] added a modifier ξ on the solar altitudes of those two extreme days. Typical values of ξ are: $\xi = 10°$ for latitudes lower than 45°N and $\xi = 5°$ for latitudes higher than 45°N. This method considered the peak delay of the thermal loads, but it is still empirical. In this case study, we used a series of solar altitudes to determine the optimal configuration through comparison. The solar altitude can be calculated according to Eqs. (3) and (4).

$$\alpha = \sin^{-1}(\cos L \cdot \cos\delta \cdot \cos h + \sin L \cdot \sin\delta) \quad (3)$$

$$\delta = 23.45 \cdot \sin\left(360 \cdot \frac{284+n}{365}\right) \quad (4)$$

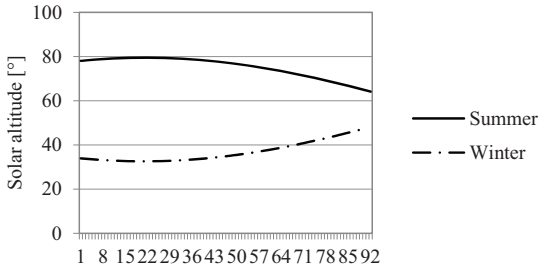

Fig. 1. Solar altitudes of Los Angeles ($L = 33.94$ N).

Table 1
d-h combinations for horizontal BISTS study (unit: m).

d	0.42	0.42	0.42	0.42	0.42	0.42	0.42	0.63	0.63	0.63	0.63	0.63
h	0.27	0.3	0.33	0.36	0.39	0.42	0.45	0.42	0.45	0.48	0.54	0.57
d	0.63	0.84	0.84	0.84	0.84	0.84	0.84	0.84	1.05	1.05	1.05	
h	0.69	0.66	0.69	0.72	0.75	0.84	0.87	0.9	0.9	0.99	1.02	

Note: d is the total horizontal depth of the BISTS; h represents the vertical height of the BISTS above the window.

where α: solar altitude [°]; δ: solar declination [°]; L: latitude of the location [°]; n: number of days in a year ($n = 1$ is the first day of a year); h: hour angle. $h = 0.25$*(number of minutes from local solar noon) [°].

Los Angeles was selected as a case study to implement the BISTS system. The summer period in Los Angeles is considered from June 1st to August 31st (92 days) in this study while the winter period is from December 1st to February 28th (90 days). The maximum summer altitude is 79.5° (June 21st) and the minimum winter solar altitude is 32.6° (December 21st), as shown in Fig. 1.

A database of 8280 *d-h* combinations was created according to Eqs. (1) and (2). However, in order to satisfy the actual panel geometry and industrial construction standard, d should be multiples of 0.21 m, and h is designed to be multiples of 0.03 m. The residuals for selecting d and h were 0.01 and 0.005 respectively. Accordingly, 23 cases were selected for Los Angeles (Table 1).

3.2.2. Vertical installation

Fig. 2(b) shows the configuration of the vertical BISTS. The distance from the wall to the central line of the panel array is 0.21 m. The shading size is determined by the shading-to-window ratio

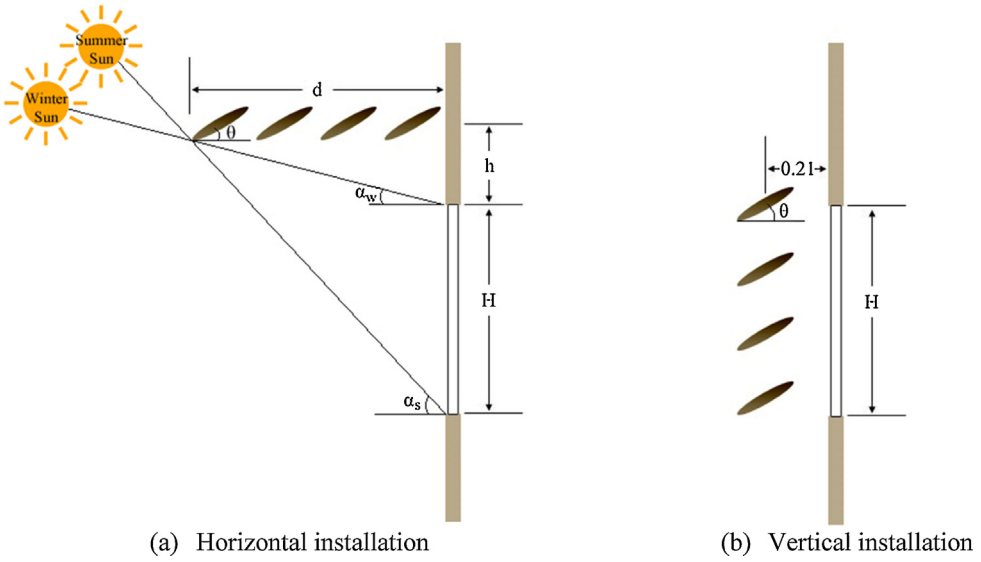

Fig. 2. BISTS configuration.

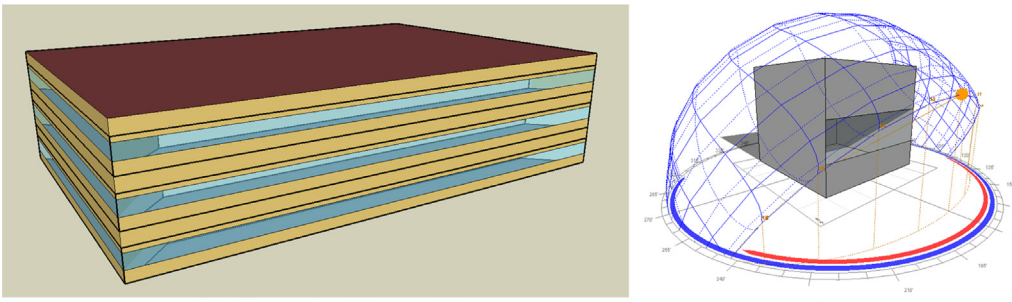

(a) Energy simulation model (b) Daylighting simulation model

Fig. 3. Building and room models.

SWR. SWR is defined as the ratio of shading area to window area, or the percentage of window area covered by shading. In this study, 2, 4, 6, and 8 panels were investigated, which correspond to the SWR of 0.32, 0.64, 0.96, and 1.28, respectively.

4. Simulation models and case study

4.1. Energy simulation model

Energy simulation was carried out in EnergyPlus based on a medium office reference building from the DOE in Los Angeles. It is a three-story building with a total floor area of 4,983 m^2 and a window fraction of 0.33, as shown in Fig. 3(a). The dimension of the building is 49.91 m (length) × 33.27 m (width) × 11.89 m (height). For the HVAC system, two-speed DX cooling coils are applied and the high speed COP is 3.23 while the low speed COP is 3.28. Natural gas is used in heating coils and the gas burner efficiency is 0.8. Electricity is consumed for reheating with an efficiency of 1. Fixed people schedule and activity level schedule are applied. The artificial lighting power is designed to be 10.76 W/m^2 (1 W/ft^2), which is compliant to baseline requirements of energy standards (ASHRAE 90.1 2004) and represents relatively efficient luminaires. A fixed lighting schedule is assigned to all lighting fixtures in the building. For the dimming control system, a daylight sensor is located at the center of each zone on the work plane. The illuminance set-point at the reference point is 500 lx. Based on the target illuminance level, the artificial lights can be continuously and linearly dimmed from maximum electric power to minimum electric power as the daylight illuminance increases. Table 2 lists the basic parameter settings for energy simulation.

Table 2
Parameter settings for energy simulation.

Occupancy density: zone floor area per person [m^2/person]	18.58
Electric equipment: watts per zone floor area [W/m^2]	10.76
Infiltration: flow per exterior surface area [m^3/s m^2]	0.000302
Outdoor air flow per person [m^3/s person]	0.0125
Heating sizing factor	1.33
Cooling sizing factor	1.33
Heating design supply air temperature [°C]	50
Heating design supply air humidity ratio [kgWater/kgDryAir]	0.008
Cooling design supply air temperature [°C]	12.8
Cooling design supply air humidity ratio [kgWater/kgDryAir]	0.0085
High speed gross rated cooling COP	3.23
Low speed gross rated cooling COP	3.28
Gas burner efficiency	0.8
Electric reheating efficiency	1
Watts per zone floor area [W/m^2]	10.76
Total building floor area [m^2]	4982.19
Building lighting level [kW]	53.6
Return air fraction	0
Fraction radiant	0.4
Fraction visible	0.2
Fraction replaceable	1
Illuminance set-point [lx]	500
Work plane height [m]	0.8

4.2. Daylighting simulation model

Daylighting simulation was conducted in DAYSIM. A single perimeter room was extracted from the medium office building as the study case. The room has a dimension of 4.57 m × 4.57 m × 3.96 m, as shown in Fig. 3(b). The window size is 4.57 m × 1.31 m and it is located 1.02 m above the floor. The reflectivity of the interior floor, ceiling, and walls are equal to 45%, 80%, and 50% respectively. A single glazed window with a visible transmittance of 0.737 was applied. The work plane is 0.8 m high from the floor and a 20 × 20 analysis grid was adopted. The analysis grid is basically an orthogonal grid of points within the model at which light, solar insolation and a range of other values can be calculated and displayed. In this study, $UDI_{500-1000}$ and $UDI_{>2000}$ values on each grid point were calculated. The average value of the total 400 points was used to represent the overall performance.

4.3. Case study

Table 3 lists the study cases investigated in this research. Each case was simulated separately so that the results can be compared to each other. The baseline case is the original medium office reference building without any BISTS devices, which provides the basic criteria for energy consumption and daylight levels. The south façade cases were integrated with horizontal BISTS layout and the configuration can be seen from Table 1. The east and west façade cases were equipped with vertical BISTS layout according to four SWRs. For each configuration, four slat angles were considered. Therefore, 92 study cases were simulated on the south façade, and 16 study cases were simulated on either east or west façade.

Table 3
Study cases (location: Los Angeles).

Case	Orientation	Installation	Configuration	Slat angle	Number of study cases
Baseline	–	–	–	–	1
BISTS	South	Horizontal	23 *d*-*h* combinations	0°, 30°, 60°, and 90°	92
	East	Vertical	4 SWRs	0°, 30°, 60°, and 90°	16
	West	Vertical	4 SWRs	0°, 30°, 60°, and 90°	16

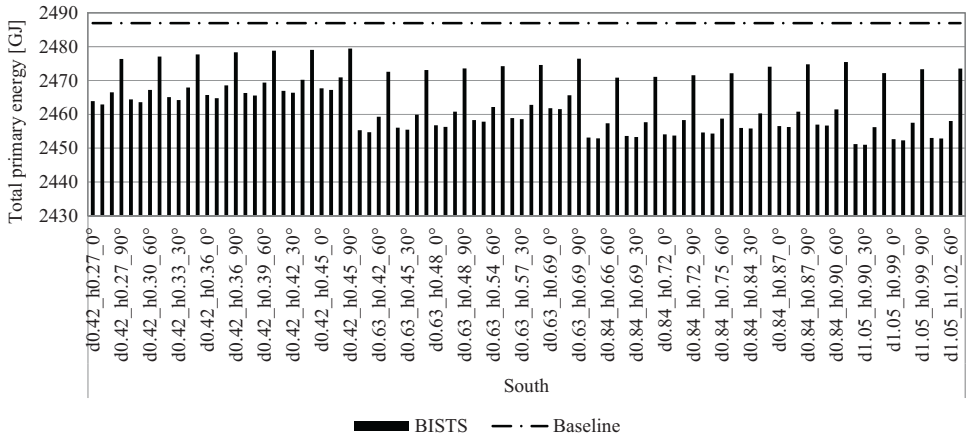

(a) Horizontal BISTS (south installation)

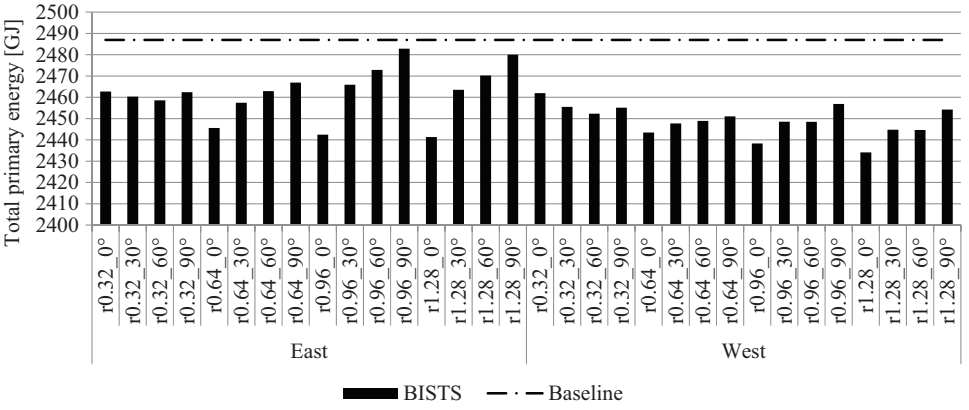

(b) Vertical BISTS (east and west installations)

Fig. 4. Energy consumption.
Note: For the case names on the x-axis, *d* is the horizontal depth of the overhang; *h* represents the vertical height of the overhang above the window; *r* is the shading-to-window ratio. For the surface slope of the solar panel, 0° is horizontal and 90° is vertical.

5. Results and comparison

5.1. Building energy consumption

The shading system can save energy by reducing the cooling loads, but could possibly increase energy needs for space heating and artificial lighting. Therefore, the overall building energy requirement needs to be investigated. Fig. 4 shows the total primary energy consumption results for the study cases with different *d*-*h* combinations, shading-to-window ratios, as well as the slat angles from 0°, 30°, 60° and 90°. *X*-axis lists the cases simulated. *Y*-axis indicates the total annual primary energy consumption in gigajoule. The horizontal dashed line represents the baseline, which is the original reference building model without any shading devices. Fig. 4(a) is the results for south façade and Fig. 4(b) includes the results for both east and west façades.

The total primary energy consumption of the baseline is about 2487 GJ. According to the prediction, all simulated cases consume less energy than the baseline, which confirms that the exterior shading is helpful to reduce the building loads. However, the savings are not significant. The south installation could save 0.3%–1.4% of total source energy. The east and west installations could save 0.2%–1.8% and 1.0%–2.1%, respectively. There are two possible reasons for the limited building energy savings. One is that the BISTS system is installed to only one façade, so that the impact to the overall energy savings of the entire building is not remarkable. Another reason is that for a large-scale building, energy consumption is mainly dominated by interior thermal loads instead of exterior weather conditions. The BISTS system mostly could influence the outdoor conditions, but not the interior loads. The best BISTS configuration on the south façade is 1.05 m deep and located at 0.9 m above the window with slat angle of 30°, which results in 1.4% of total primary energy saving from the baseline (Table 4). On the east and west façades, the best cases have the same configuration: 1.28 of SWR and 0° of slat angle, which reduce the total primary energy consumption by 1.8% (east) and 2.1% (west). The western

Table 4
Comparison of primary energy consumption for the baseline and the best cases on each façade.

Orientation	Case name	Reheating Ele [GJ]	Cooling Ele [GJ]	Interior lights [GJ]	Heating gas [GJ]	Total [GJ]	Δ Total [%]
–	Baseline	169.34	787.02	1530.44	0.13	2486.94	–
South	d1.05_h0.90_30°	160.17	759.62	1531.03	0.20	2451.02	−1.4
East	r1.28_0°	142.82	756.16	1542.11	0.22	2441.32	−1.8
West	r1.28_0°	138.68	753.06	1542.17	0.22	2434.13	−2.1

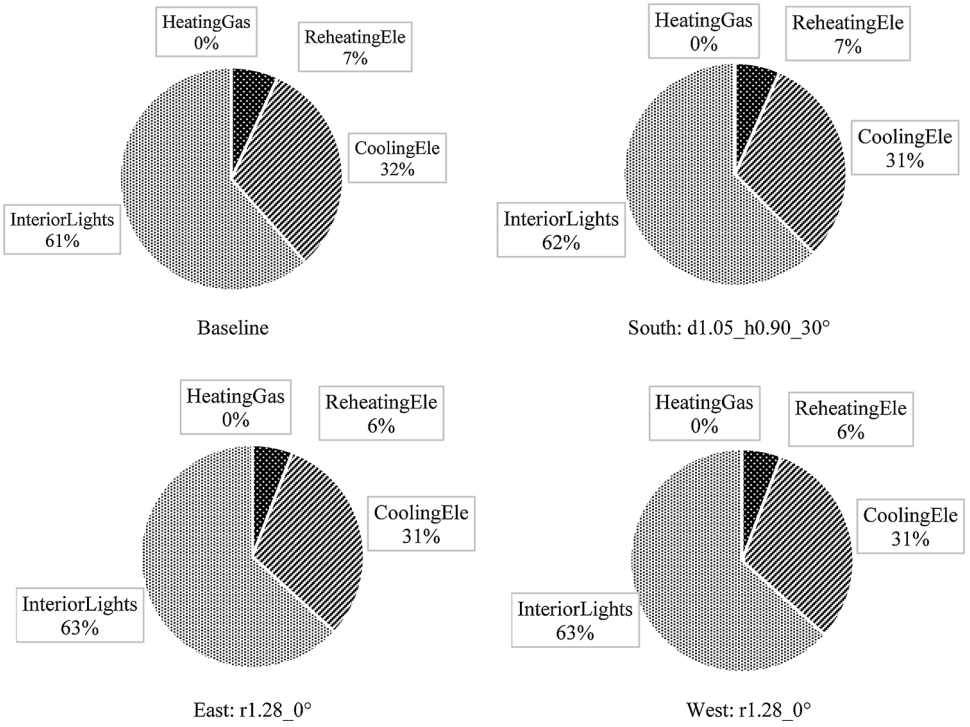

Fig. 5. Energy consumption breakdown of the baseline and the best cases on each façade.

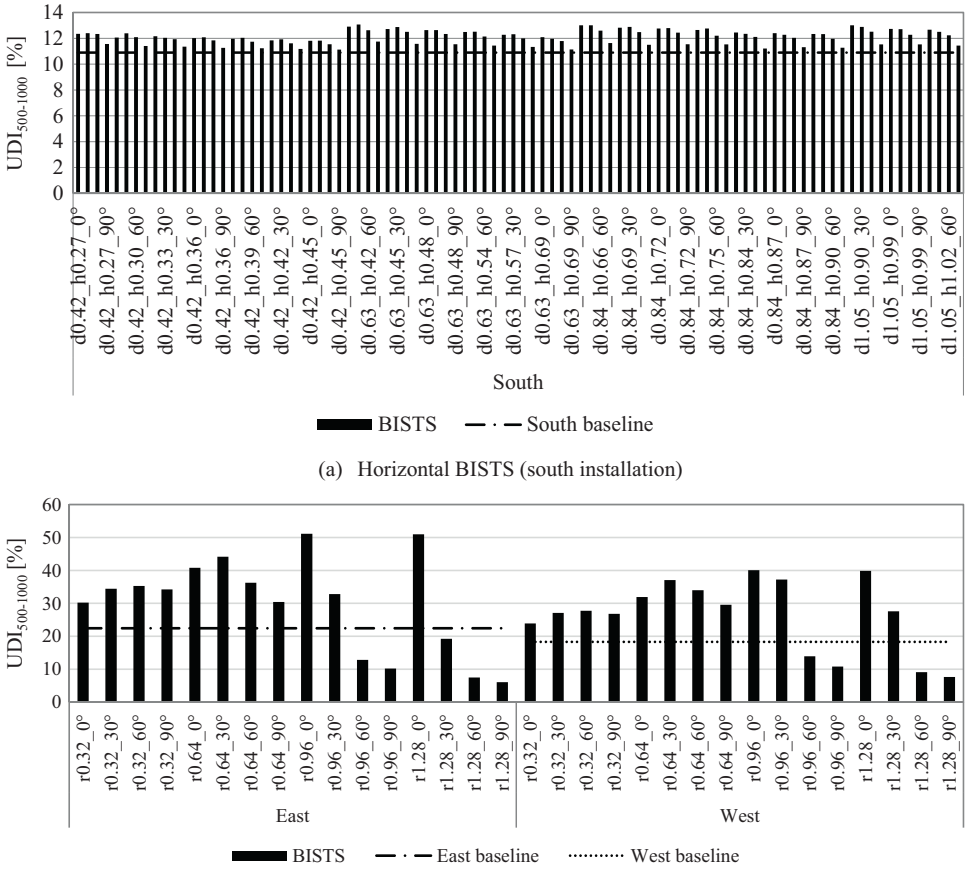

(a) Horizontal BISTS (south installation)

(b) Vertical BISTS (east/west installation)

Fig. 6. $UDI_{500–1000}$ level.

BISTS installation has better potential on energy saving than the eastern one because the outdoor temperature and the cooling load are higher in the afternoon. The west BISTS can block the solar radiation and reduce the solar gain, so that it can save more energy from space cooling.

Energy consumed by interior lighting and space cooling constitutes the majority of the total consumption (Fig. 5). Interior lighting accounts for more than 60% of primary energy, while space cooling accounts for around 30%. The gas consumption for space heating is negligible. The BISTS system increases the energy consumption for artificial lighting and space heating because it blocks the sunlight, so that reduces the solar availability to light and heat the building. However, the increment is not significant and can be easily offset by the energy savings from space cooling and reheating; therefore the total energy consumption is reduced.

Slat angle could also influence the energy performance. 90° does not work well for all cases. Smaller angles have better performance. For the horizontal BISTS on the south façade, the results change markedly when the slat angle increases from 60° to 90°. Therefore, slat angles greater than 60° are not recommended for horizontal BISTS configuration.

5.2. $UDI_{500-1000}$ level

A higher $UDI_{500-1000}$ level is desired by the occupants because it could provide adequate light without compensation from artificial lighting and avoid causing visual discomfort. On the south façade, all studied BISTS cases can increase the values of $UDI_{500-1000}$ compared to the baseline data, as shown in Fig. 6(a). The best case improves the $UDI_{500-1000}$ value from 11% to 13%. 30° slat angle works best for most cases. On the east and west façades, smaller SWR cases such as r0.32 and r0.64 can always increase the $UDI_{500-1000}$ levels. On the other hand, for the larger SWR cases, like r0.96 and r1.28, the performance of BISTS is highly dependent on slat angles. Smaller slat angles can impressively improve the values of $UDI_{500-1000}$ but larger slat angles reduce the $UDI_{500-1000}$ levels dramatically. Thus, the combinations of large SWR and small slat angle could be better options. For instance, case "r0.96_0°" increases the $UDI_{500-1000}$ value from 22% to 51% on the east façade, and from 18% to 40% on the west façade, as listed in Table 5.

A more visualized comparison would be the spatial distribution of the annual average $UDI_{500-1000}$ on the work plane. This is presented in Fig. 7. The contour plots show that: 1) for the south window orientation, the BISTS installation slightly influences the interior $UDI_{500-1000}$ distribution. Only in the deeper room is a slight increase in the useful daylight level realized. This is because the horizontal BISTS allows the sunlight to come through during the winter season, thus rarely influencing the interior daylighting condition. 2) For the east and west window orientations, since the best cases fully cover the window and affect the interior illuminance all year round, the $UDI_{500-1000}$ distribution is greatly skewed. Although the overall useful daylight level is significantly improved, the distribution is not uniform. 3) The southwest corner has higher $UDI_{500-1000}$ level for the east orientation. The southeast corner, though, has better useful daylight condition for the west orientation.

Another way to determine the optimal spatial area is to plot the average $UDI_{500-1000}$ as a function of distance from the window. Fig. 8 displays the comparison of the baselines and the best cases.

Table 5
Best cases for $UDI_{500-1000}$ improvement.

Orientation	Case name	$UDI_{500-1000}$ [%]	Baseline [%]	Δ $UDI_{500-1000}$ [%]
South	d0.63_h0.42_30°	13.1	10.9	+2.2
East	r0.96_0°	51.1	22.4	+28.7
West	r0.96_0°	40.1	18.3	+21.8

Each point on this graph is the average value of $UDI_{500-1000}$ at the grid points on the work plane that have the same horizontal distance from the window. It indicates that the useful daylight level minimizes at about 0.6 m from the window, and reaches the peak at around 4.5 m and 3 m of distance from the window for the room oriented at south and east/west, respectively. This implies that 4.5 m and 3 m away from the window would be the best areas to receive most useful daylight, depending on the window orientation.

5.3. $UDI_{>2000}$ level

Higher $UDI_{500-1000}$ level does not necessarily mean better daylighting performance. Too much illuminance on the work plane could potentially cause glare problems. Therefore, $UDI_{>2000}$ level should also be investigated to prevent from excessive daylight. The simulation results indicate that all studied cases could reduce the values of $UDI_{>2000}$ from the baseline (Fig. 9). The best case on the south façade reduces the $UDI_{>2000}$ value by 6% while the best cases on the east and west façades could reduce the $UDI_{>2000}$ values by more than 30%, as listed in Table 6. For the horizontal BISTS configuration, 30° slat angle works best for most cases, but 90° is not recommended. For the vertical BISTS, 60° slat angle is the best choice for all cases, but 0° does not work well. The combinations of high SWR and large slat angle can achieve better $UDI_{>2000}$ level reduction.

It can be predicted that the closer to the window, the higher daylight illuminance appears. This is reflected in Fig. 10, which displays the spatial distribution of annual average $UDI_{>2000}$ levels on the work plane. The east and west BISTS installations could reduce excessive daylight more effective than south installation. Lower $UDI_{>2000}$ levels occur at the southwest corner for the east orientation, and at the southeast corner for the west orientation. Considering the results of $UDI_{500-1000}$ level, these two corners would be the optimal areas for daylighting condition. Fig. 11 indicates that the $UDI_{>2000}$ level maximizes at about 0.6 m from the window and then decreases in the deeper room. Thus, the "risky" areas are around 0.6 m of distance from the window, but it should note that 2000 lx does not necessarily mean visual discomfort and positions closer to the window could also be acceptable [33].

6. Discussion

6.1. Final proposed BISTS configuration

It is not always possible to achieve the best energy saving and daylight provision by using the same BISTS configuration. Compromise is necessary to propose a final design. In this study, primary energy saving, $UDI_{500-1000}$ level, and $UDI_{>2000}$ level are three evaluated indicators. For multi-objective optimization, the decision-making is depending on the preference of the user. Usually we give weight for each indicator to represent the preferences. It is noticed that the interior daylight levels of a perimeter room can be significantly improved due to the BISTS application, but the influence to the building energy consumption is very slight. Therefore, more weight was given to the daylighting performance to determine the final design.

For the horizontal BISTS, case "d0.84_h0.66_30°" was selected for the south façade because it shows outstanding performances on $UDI_{>2000}$ reduction and $UDI_{500-1000}$ improvement, as well as notable performance on primary energy saving. For the vertical BISTS, it was recommended to fully cover the window, and 0° slat angle helps to redirect the sunlight into the deeper room. Thus, case "r1.28_0°" was used for both east and west façades. Fig. 12 and Table 7 display the final BISTS configuration. It consists of 12 strip panels on the south façade, in which 4 panels are placed in a

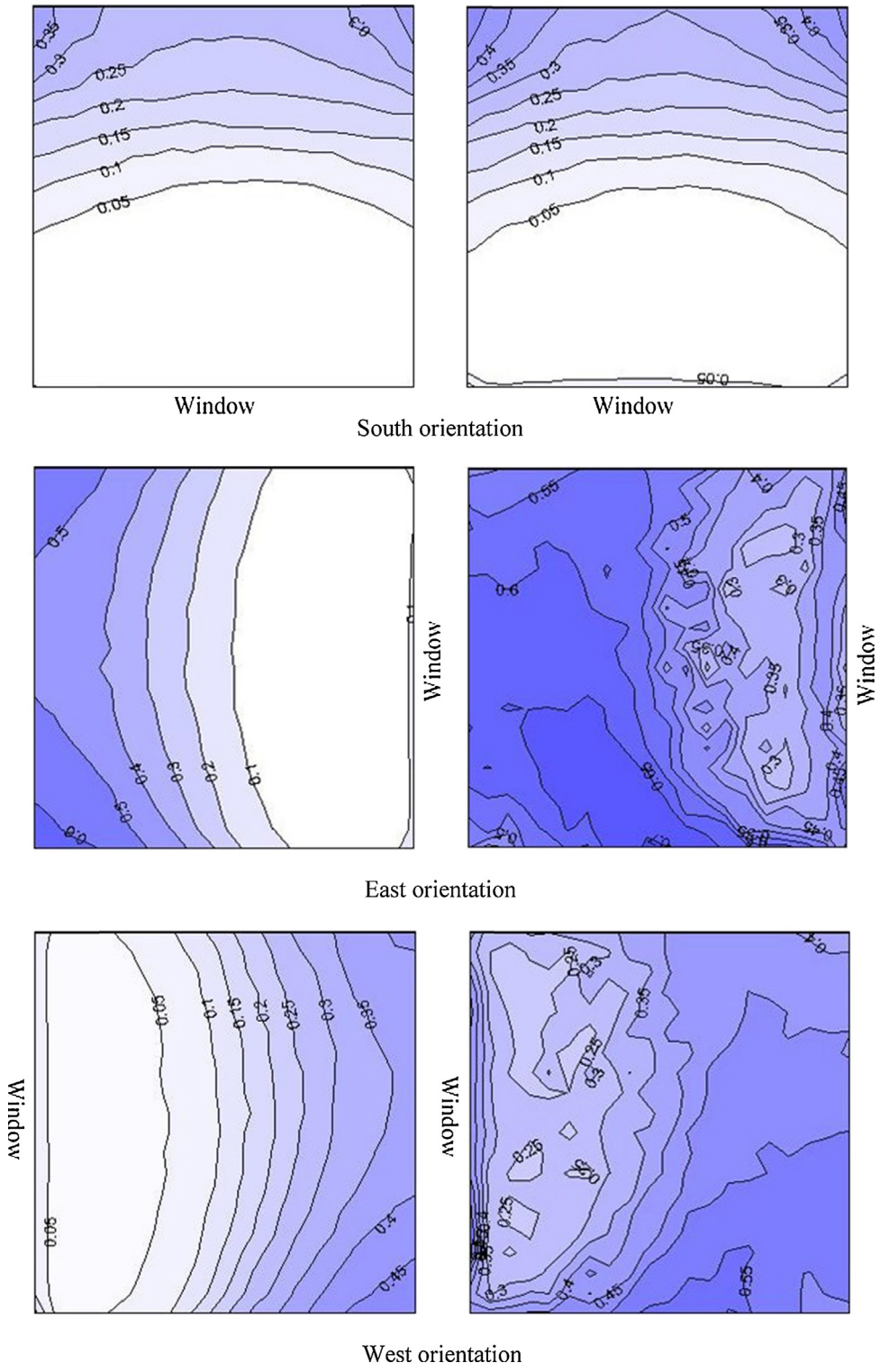

Fig. 7. Spatial distribution of annual average $UDI_{500-1000}$ level for the baselines (left) and the best cases (right) of each window orientation.

horizontal array on each strip window with 30° surface slope. The total depth of the BISTS is 0.84 m and it is located 0.66 m above the window. The total collector area on the south façade is about 125 m^2. On the east and west façades, 48 panels are symmetrically mounted in vertical arrays with 0° slat angle (8 panels on each strip window). The shading-to-window ratio is 1.28 and the collector area is 167.5 m^2 for each side. To sum up, the total collector area installed to the building is about 460 m^2.

6.2. Performance

The total building energy consumption of the medium office with the final BISTS configuration was predicted and shown in Fig. 13. The total primary energy saving due to the BISTS application is 131.4 GJ, which is about 5.3% of the baseline consumption. Interior artificial lighting counts for more than half of the primary energy. Space cooling contributes most, 90.3 GJ, to the total savings.

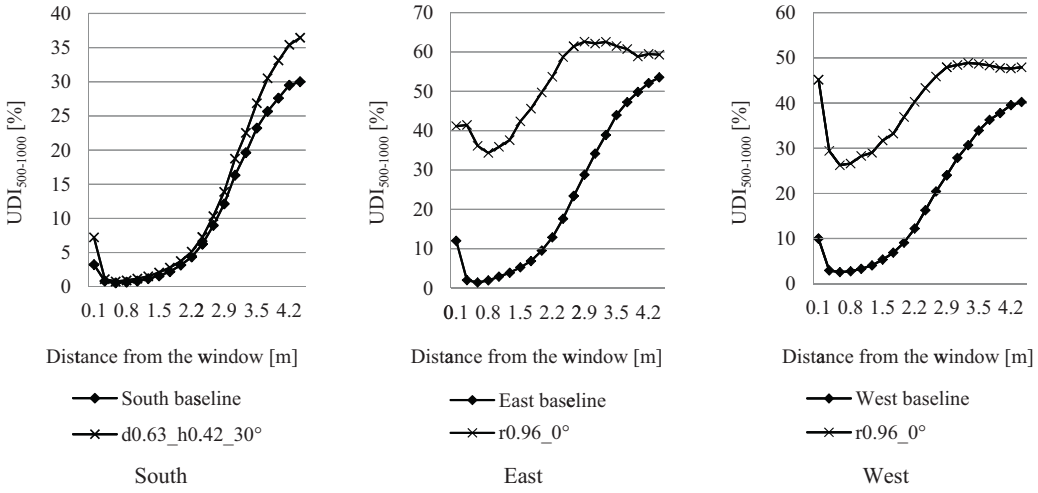

Fig. 8. $UDI_{500–1000}$ level distribution on the work plane as a function of the distance from the window for the baselines and the best cases of each window orientation.

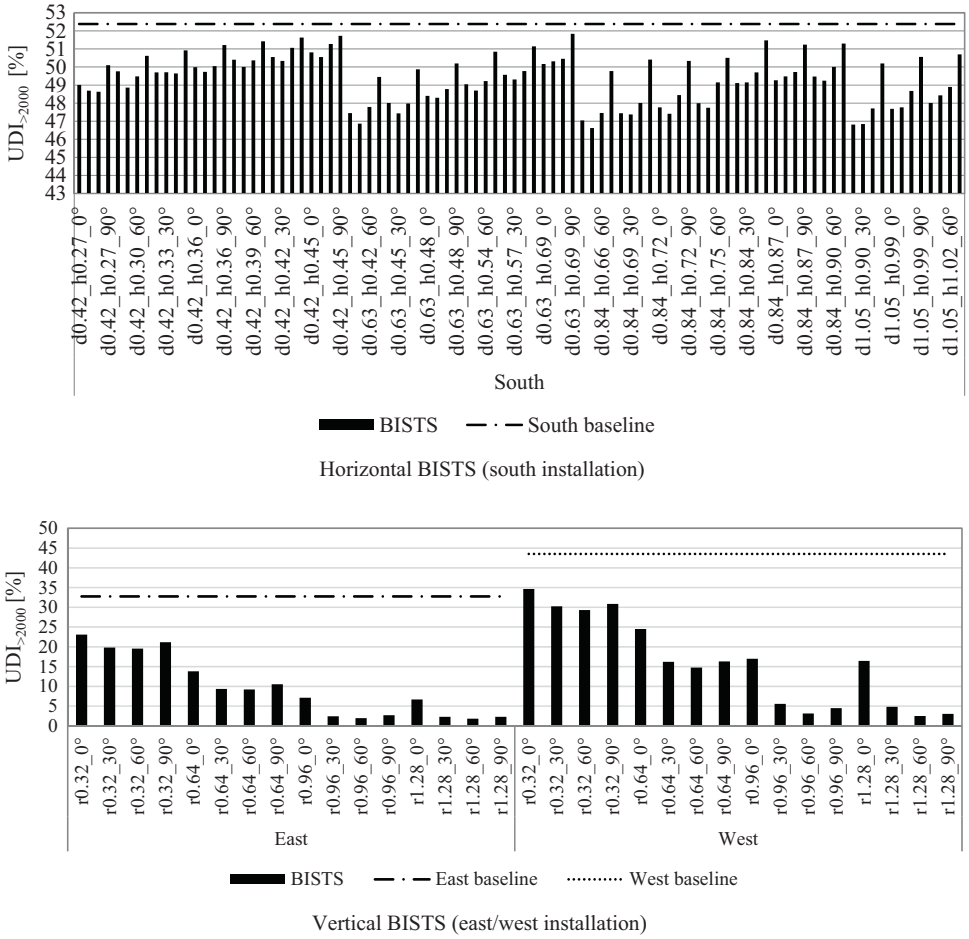

Fig. 9. $UDI_{>2000}$ level.

Table 6
Best cases for $UDI_{>2000}$ reduction.

Orientation	Case name	$UDI_{>2000}$ [%]	Baseline [%]	Δ $UDI_{>2000}$ [%]
South	d0.84_h0.66_30°	46.6	52.4	−5.8
East	r1.28_60°	1.8	32.8	−30.9
West	r1.28_60°	2.5	43.5	−41.0

As noticed in Fig. 14, the building in Los Angeles has cooling load all year round.

The daylight level performance of the final BISTS configuration is displayed in Fig. 15. It increases the $UDI_{500–1000}$ level from the baseline by 2.1%, 28.5%, and 21.6% for the south, east, and west oriented rooms, respectively, and reduces the $UDI_{>2000}$ level by 5.8% (south), 26.1% (east), and 27.0% (west).

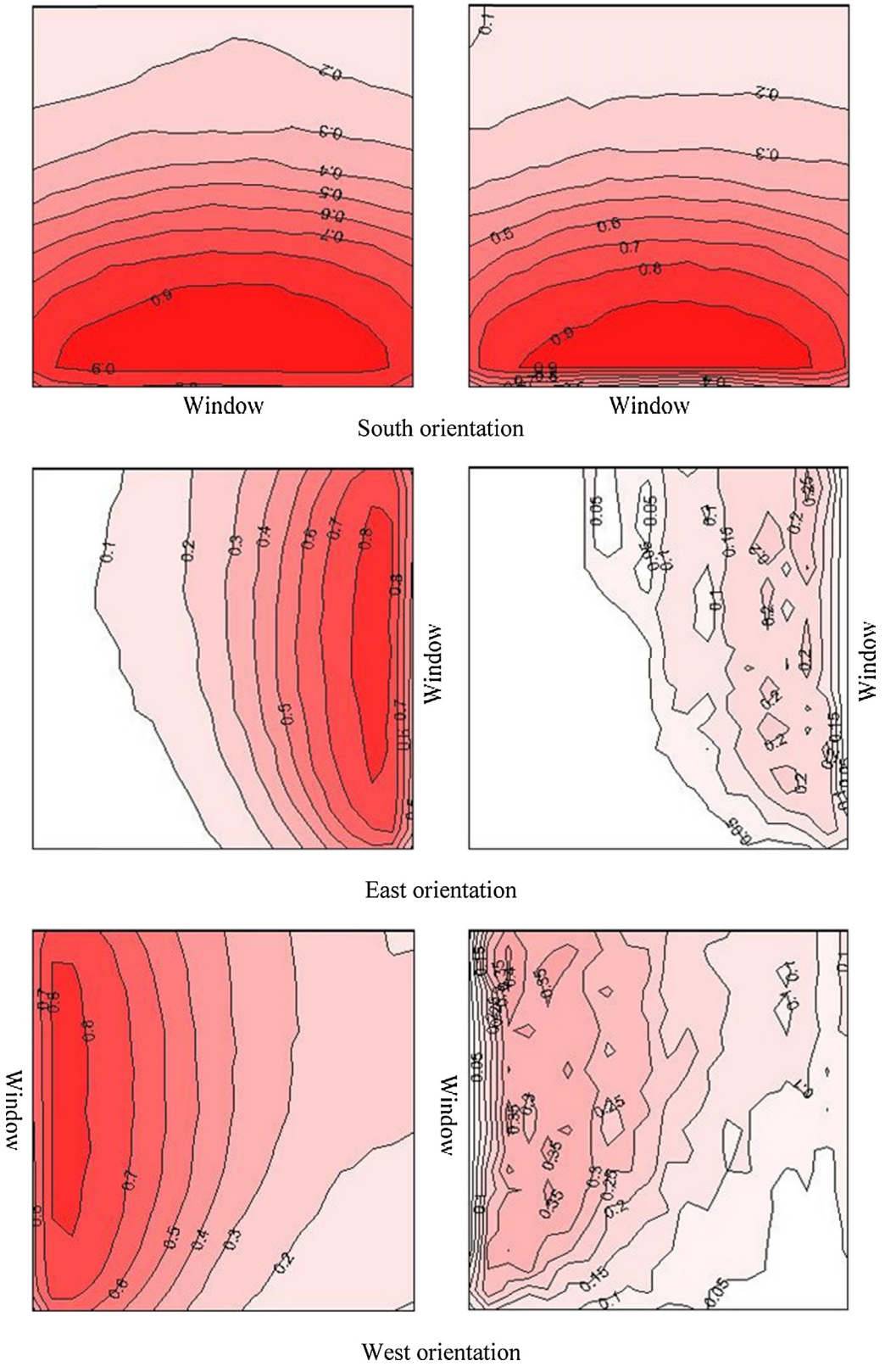

Fig. 10. Spatial distribution of annual average $UDI_{>2000}$ level for the baselines (left) and the best cases (right) of each window orientation.

6.3. Cost analysis

The payback period can be simply calculated by considering the initial investment $C_{initial}$ for a given collector area and the annual savings. The manufacturer reported that the price of the BISTS system is about \$65 m^{-2}. $C_{initial}$ of the final BISTS configuration, therefore, would be \$29,900. Cost savings of the BISTS application come from the reduction of electricity and natural gas consumption, not only by passively influencing the heating, cooling, and artificial lighting loads, as discussed above in this paper, but also by

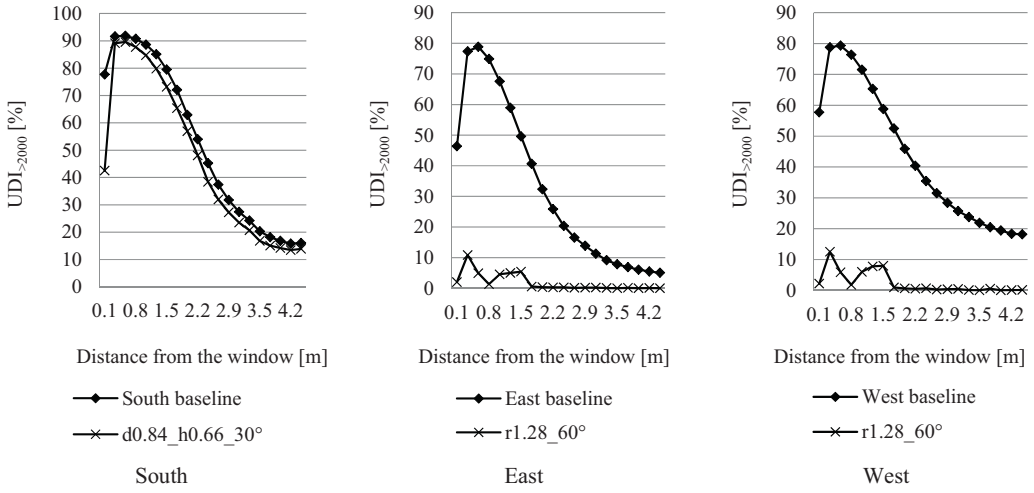

Fig. 11. $UDI_{>2000}$ level distribution on the work plane as a function of the distance from the window for the baselines and the best cases of each window orientation.

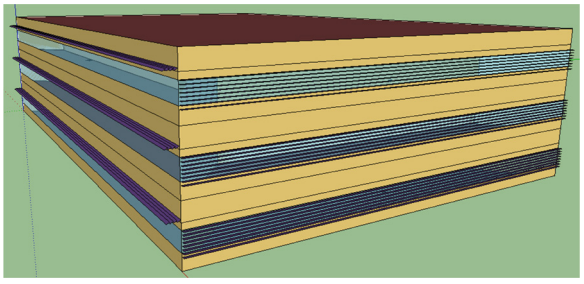

Fig. 12. Final BISTS configuration.

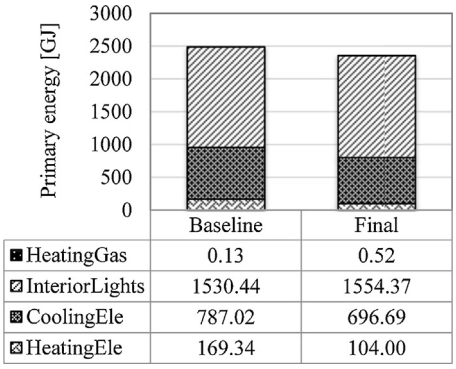

Fig. 13. Primary energy consumption of the building with the final BISTS configuration.

Table 7
Final BISTS configuration.

Orientation	Configuration	Number of panels	Slat angle	Collector area [m^2]
South	d0.84_h0.66_30°	12	30°	125
East	r1.28_0°	24	0°	167.5
West	r1.28_0°	24	0°	167.5
Total		60		460

actively providing free solar energy for domestic hot water (DHW) and space heating. Further investigation concluded that the proposed BISTS system is able to serve 75.5% of the domestic hot water load, and provide 64.6% of the space heating demand [34]. According to the U.S. Energy Information Administration, the electricity price in California is \$0.1813 kWh^{-1}, and the natural gas price is

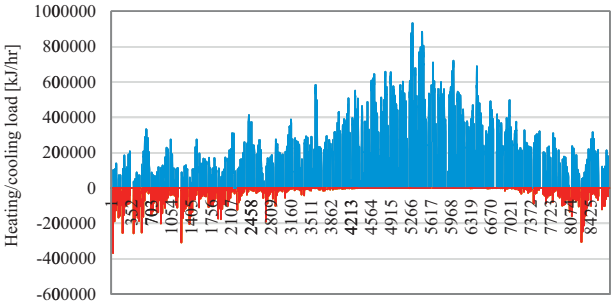

Fig. 14. Annual space heating and cooling loads of the building with the final BISTS configuration.

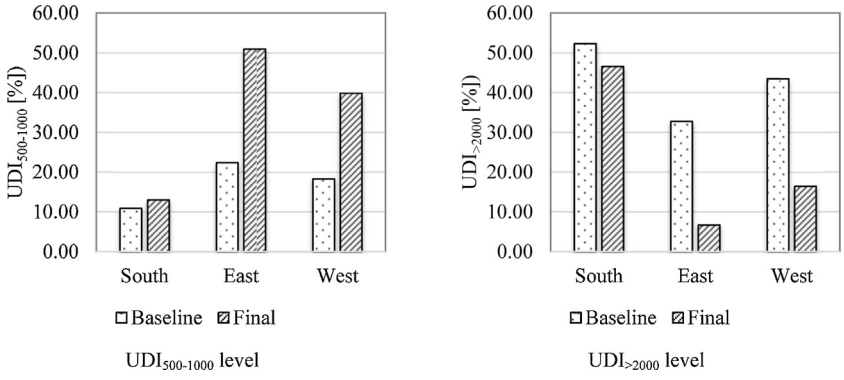

Fig. 15. UDI levels of the room with the final BISTS configuration.

Table 8
Cost analysis of the proposed BISTS configuration.

$C_{initial}$ [$]	Annual site energy savings									Annual cost saving [$]	Payback [yr]
	Passive saving		DHW saving		Space heating saving			Total saving			
	Ele [kWh]	Gas [ft^3]	F_{solar} [%]	Gas [ft^3]	F_{solar} [%]	Ele [kWh]	Gas [ft^3]	Ele [kWh]	Gas [ft^3]		
29900	11824.6	−326.0	75.5	25456.4	64.6	6029.8	282.6	17854.4	25412.9	3538.1	8.5

$0.01185 ft^{-3}. Table 8 lists the annual energy and cost savings. The payback period is calculated to be 8.5 years.

7. Conclusion

This study focused on the performance evaluation of the BISTS system on building energy consumption and daylight levels when it is applied to a medium office reference building in Los Angeles. The following conclusions were achieved:

First, the BISTS system helps to reduce the building energy consumption. All simulated cases showed energy savings compared with the baseline. The savings vary for different BISTS configurations. The results revealed that 1.4% of primary energy saving can be obtained due to the south horizontal BISTS installation. 1.8% and 2.1% of energy savings can be achieved from the east and west vertical BISTS installations, respectively. The energy saving is not very significant because 1) the BISTS system is installed to only one façade so that the impact on the overall energy consumption of the entire building is limited; 2) for a large-scale building, energy consumption is mainly dominated by interior loads instead of weather condition.

Secondly, the BISTS system improves the interior useful daylight level and reduces the excessive daylight level for a single perimeter room. The best cases increase the $UDI_{500–1000}$ value by 2.2%, 28.7%, and 21.8% for the south-facing, east-facing, and west-facing rooms, respectively and reduce the $UDI_{>2000}$ value by 5.8% (south), 30.9% (east), and 41.0% (west). However, some vertical cases with high SWRs and large slat angles cannot benefit the useful daylight, which should be avoided for applications. The BISTS system also changes the illuminance distribution on the work plane, especially for the east and west installations.

Third, the final BISTS design combines the BISTS application on three façades and leverages the performances of primary energy saving and daylight provision. The final proposed design could save 5.3% of the total primary energy and increase the $UDI_{500–1000}$ value by 2.1% (south), 28.5% (east), and 21.6% (west). It could also reduce the $UDI_{>2000}$ value by 5.8% (south), 26.1% (east), and 27.0% (west).

Finally, slat angle influences the BISTS louver performance. For both horizontal and vertical BISTS layouts, 90° slat angle should be avoided in consideration of energy saving and useful daylight. Small slat angles are recommended for horizontal BISTS because when the slat angle increases from 60° to 90°, the results become markedly undesirable. 0° slat angle is more preferred for vertical BISTS because it increases the daylight availability in the deeper space of the room.

References

[1] C. Lamnatou, J.D. Mondol, D. Chemisana, C. Maurer, Modelling and simulation of Building-Integrated solar thermal systems: behaviour of the system, Renew. Sustain. Energy Rev. 45 (2015) 36–51.
[2] 2011 Buildings Energy Data Book, U.S. Department of Energy, 2012, Available: http://buildingsdatabook.eren.doe.gov/default.aspx (accessed 8.3.15).
[3] C. Lamnatou, J.D. Mondol, D. Chemisana, C. Maurer, Modelling and simulation of Building-Integrated solar thermal systems: behaviour of the coupled building/system configuration, Renew. Sustain. Energy Rev. 48 (2015) 178–191.
[4] X.-Y. Sun, X.-D. Sun, X.-G. Li, Z.-Q. Wang, J. He, Performance and building integration of all-ceramic solar collectors, Energy Build. 75 (2014) 176–180.
[5] M.M. Hassan, Y. Beliveau, Design, construction and performance prediction of integrated solar roof collectors using finite element analysis, Constr. Build. Mater. 21 (2007) 1069–1078.
[6] C. Maurer, T. Baumann, M. Hermann, P.D. Lauro, S. Pavan, L. Michel, T.E. Kuhn, Heating and cooling in high-rise buildings using facade-integrated transparent solar thermal collector systems, J. Build. Perform. Simul. 6 (6) (2013) 449–457.
[7] T. Matuska, B. Sourek, Facade solar collectors, Sol. Energy 80 (2006) 1443–1452.
[8] C. Lamnatou, G. Notton, D. Chemisana, C. Cristofari, The environmental performance of a building-integrated solar thermal collector, based on multiple approaches and life-cycle impact assessment methodologies, Build. Environ. 87 (2015) 45–58.
[9] C. Lamnatou, G. Notton, D. Chemisana, C. Cristofari, Life cycle analysis of a building-integrated solar thermal collector, based on embodied energy and embodied carbon methodologies, Energy Build. 84 (2014) 378–387.
[10] F. Motte, G. Notton, C. Cristofari, J.-L. Canaletti, A building integrated solar collector: performance characterization and first stage of numerical calculation, Renew. Energy 49 (2013) 1–5.
[11] A.I. Palmero-Marrero, A.C. Oliveira, Effect of louver shading devices on building energy requirements, Appl. Energy 87 (2010) 2040–2049.
[12] A.I. Palmero-Marrero, A.C. Oliveira, Evaluation of a solar thermal system using building louvre shading devices, Sol. Energy 80 (2006) 545–554.
[13] M.C. Dubios, Solar Shading and Building Energy Use, Lund University, Lund, 1997.
[14] S. Citherlet, J.A. Clarke, J. Hand, Integration in building physics simulation, Energy Build. 33 (2001) 451–461.
[15] S. Kota, J.S. Haberl, Historical survey of daylighting calculations methods and their use in energy performance simulations, in: Proceedings of the Ninth International Conference for Enhanced Building Operations, Austion, Texas, 2009, Vols. ESL-IC-09-11-07.
[16] M. Mandalaki, K. Zervas, T. Tsoutsos, A. Vazakas, Assessment of fixed shading devices with integrated PV for efficient energy use, Sol. Energy 86 (2012) 2561–2575.
[17] M. Mandalaki, T. Tsoutsos, N. Papamanolis, Integrated PV in shading systems for Mediterranean countries: balance between energy production and visual comfort, Energy Build. 77 (2014) 445–456.
[18] H. Van Dijk, Reference Office for Thermal, Solar and Lighting Calculations, IEA Task 27, Performance of Solar Facades Components, TNO Building and Construction Research, Delft, The Netherlands, 2011.
[19] M. Manzan, Genetic optimization of external fixed shading devices, Energy Build. 72 (2014) 431–440.
[20] H. Shen, A. Tzempelikos, Daylighting and energy analysis of private offices with automated interior roller shades, Sol. Energy 86 (2012) 681–704.
[21] Y.-C. Chan, A. Tzempelikos, Efficient venetian blind control strategies considering daylight utilization and glare protection, Sol. Energy 98 (2013) 241–254.
[22] Y.-C. Chan, A. Tzempelikos, A hybrid ray-tracing and radiosity method for calculating radiation transport and illuminance distribution in spaces with venetian blinds, Sol. Energy 86 (2012) 3109–3124.
[23] "Commercial Reference Buildings," Office of Energy Efficiency & Renewable Energy, U.S. Department of Energy. Available: http://energy.gov/eere/buildings/commercial-reference-buildings (accessed 14.7.15).
[24] R.A. Athalye, Y. Xie, B. Liu, M.I. Rosenberg, Analysis of Daylighting Requirements within ASHRAE Standard 90.1, Pacific Northwest National Laboratory, Richland, Washington 99352, 2013.
[25] EnergyPlus Energy Simulation Software: About EnergyPlus, 2015, Available: http://apps1.eere.energy.gov/buildings/energyplus/energyplus_about.cfm (accessed 1.3.15).
[26] "The difference between source and site energy," Energy Star. Available: http://www.energystar.gov/buildings/facility-owners-and-managers/existing-buildings/use-portfolio-manager/understand-metrics/difference (accessed 5.8.15).
[27] C.F. Reinhart, O. Walkenhorst, Validation of dynamic RADIANCE-based daylight simulations for a test office with external blinds, Energy Build. 33 (2001) 683–697.

[28] DAYSIM, 2015, Available: http://daysim.ning.com/ (accessed 1.3.15).
[29] A. Nabil, J. Mardaljevic, Useful daylight illuminances: a replacement for daylight factors, Energy Build. 38 (7) (2006) 905–913.
[30] A. Nabil, J. Mardaljevic, Useful daylight illuminance: a new paradigm for assessing daylight in buildings, Lighting Res. Technol. 37 (1) (2005) 41–59.
[31] A.B. Sawant, R.V. Jugdar, S.G. Sawant, Light transmitting concrete by using optical fiber, Int. J. Invent. Eng. Sci. 3 (1) (2014).
[32] S. Raeissi, M. Taheri, Optimum overhang dimensions for energy saving, Build. Environ. 3 (5) (1998) 293–302.
[33] A. Tzempelikos, H. Shen, Comparative control strategies for roller shades with respect to daylighting and energy performance, Build. Environ. 67 (2013) 179–192.
[34] L. Li, M. Qu, S. Peng, Performance evaluation of building integrated solarthermal shading system: active solar energy usage, Energy Build. (under revision).